Received: 10 May 2017 | Revised: 24 August 2017 | Accepted: 1 September 2017

DOI: 10.1111/ffe.12721

ORIGINAL CONTRIBUTION

WILEY

Fatigue characterization of T300/924 polymer composites with voids under tension-tension and compression-compression cyclic loading

H. Liu[1] | H. Cui[1,2] | W. Wen[1,2] | H. Kang[3]

[1]College of Energy and Power Engineering, Nanjing University of Aeronautics and Astronautics, Nanjing, China

[2]State Key Laboratory of Mechanics and Control of Mechanical Structures, Nanjing University of Aeronautics and Astronautics, Nanjing, China

[3]College of Engineering and Computer Science, University of Michigan-Dearborn, Dearborn, MI, USA

Correspondence
H. Liu, College of Energy and Power Engineering, Nanjing University of Aeronautics and Astronautics, 29 Yudao St, Nanjing 210016, China.
Email: haolongl@umich.edu

Abstract

Fibrous polymer composites exhibit excellent properties such as high specific stiffness/strength and good fatigue performance. However, as inherent defects of polymer composites, voids have been reported to have an impact on their load-bearing properties including fatigue resistance. In the interest of safety, the effect of voids on fatigue behaviours of composites should be understood and quantified. In this article, the effect of voids on the fatigue of T300/924 composites was evaluated in terms of their fatigue life, stiffness degradation, and cracks propagation under tension-tension and compression-compression loadings. The failure probability was assessed by Weibull distribution. Furthermore, crack measurement and fractographic analysis reveal that the effect of voids on the failure mechanisms of the material under various loading configurations could be different. Lastly, an analytical residual stiffness model was proposed, and a good correlation was obtained between the experimental data and the prediction results.

KEYWORDS

crack density measurement, effect of voids, fatigue behaviours, polymer composite

Nomenclature: R, = stress ratio; u, = stress level; v_v, = void content; N_f, = fatigue life; i, = serial number of samples; n, = number of cycles; $\eta(u)$, = scale parameter of Weibull distribution; $\lambda(u)$, = shape parameter of Weibull distribution; $P(n_i)$, = failure probability of the no. i, sample after n, cycles; $[\sigma_t]$, = tensile strength; $[\sigma_c]$, = compressive strength; a, = normalized stress amplitude; q, = normalized mean stress; c, = ratio between compressive strength and tensile strength; A, f, = constants associated with material; $\gamma(v_v)$, = intercept of $S-N$, curve with vertical axis (for composite with void content of v_v,); $k(v_v)$, = slope of $S-N$, curve (for composite with void content of v_v,); σ_{max}, σ_{min}, = maximum and minimum stress of cyclic load; D, = fatigue damage index; E_0, = initial modulus; $E(N)$, = residual modulus of the N^{th}, cycle; $E(N_f)$, = modulus at final fracture; $\delta(u, v_v)$, $\varphi_i(u, v_v)$, = functions related to the characteristics of damage accumulation ($i \in$, 1,2)

1 | INTRODUCTION

For the last decades, a growing interest has been seen in extensive use of carbon fibre reinforced polymer (CFRP) composites in a wide range of manufacturing industries. As low weight has become one of the most urgent targets for both vehicles and airplanes in meeting customer demands and government regulations for energy efficiency, the situation can be improved with the implementation of CFRP composites because of their many advantages in terms of high strength-to-density ratio and good fatigue resistance. Vast amount of works have been

done to investigate the mechanical properties of polymer composites; however, some of the work revealed that the voids have an impact on the mechanical properties, especially fatigue performance.[1-10]

It has been commonly accepted that the fatigue process of composites is totally different and more complicated compared with that of metals. The complexity derives from different failure mechanisms, which are influenced by several factors according to previous studies: (1) mechanical properties of the material components, such as fibre, matrix, and fibre-matrix interface[11]; (2) fibre orientation and fibre volume fraction[12,13]; and (3) manufacturing defects and material aging due to the extreme working conditions (eg, fibre defects,[14] voids,[1-10] and mechanical degradation due to hygrothermal aging[15] or ultraviolet radiation[16]). Among these factors, voids, as one of the most common defects in resin polymer composites, are inevitably induced during manufacturing process. Many researchers devoted to investigating the formation mechanisms of voids,[17,18] the effect of voids on the quasistatic properties,[19-21] and the fatigue properties of composites.[1-10]

As early as 1981, the effect of voids on composite structures has drawn attentions of researchers. Garbo and Ogonowski[1] investigated the effect of voids on the fatigue of composite joints, and they stated that up to moderate porosity, the presence of voids has limited effect on the fatigue life of the joint. In the same year, R. Prakash[2] studied fatigue fracture surfaces of HM-S/828 composite using a scanning electron microscope (SEM); a failure hypothesis for composites with the presence of defects (voids, etc) was put forward based on the fractographic evidences. Since then, the effects of voids on fatigue behaviours of composite materials were studied by researchers across the world.[3-10] De Almeida[3] investigated the effect of voids on the flexural fatigue of AS4/PMR-15 composite; a strong detrimental effect on the fatigue performance of the composite structure was observed when the void content was above a critical value. J. Lambert[4] characterized the voids and their

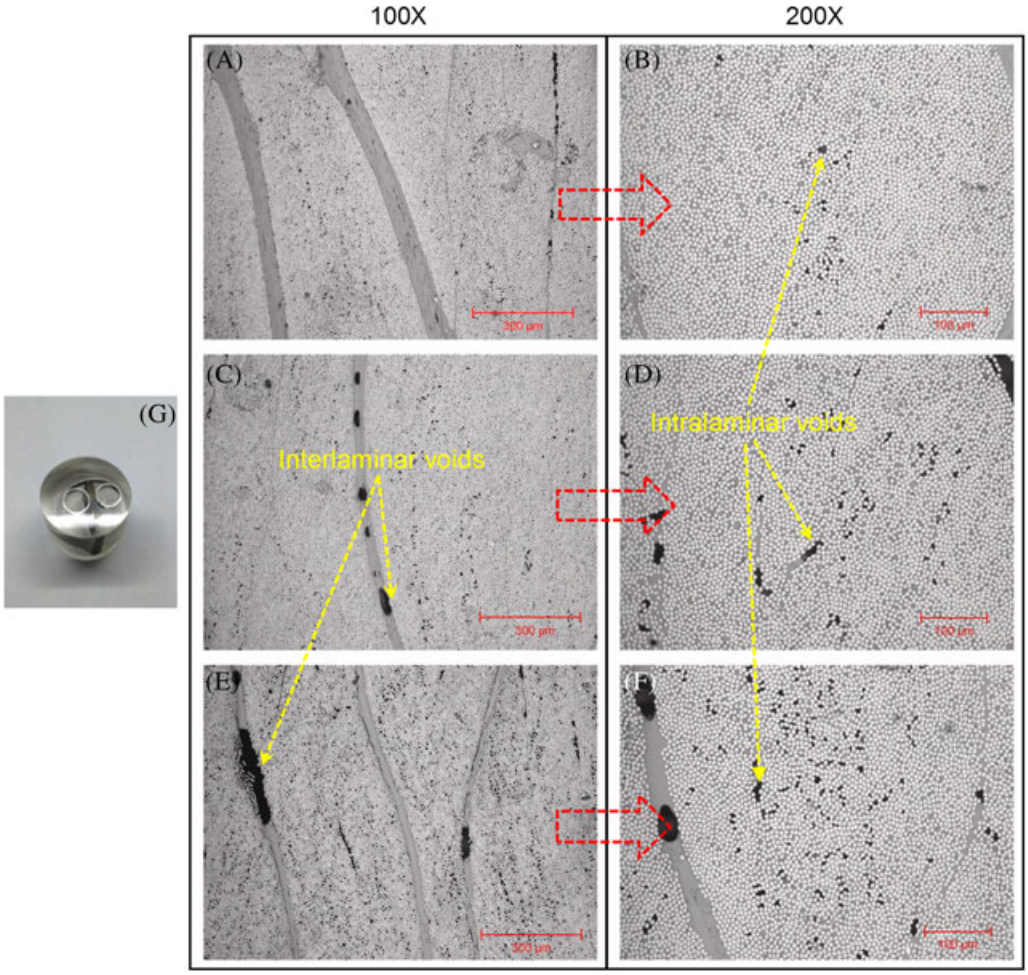

FIGURE 1 Cross-sectional images of unidirectional composite laminates obtained by optical microscope. A,B, Cured at 0.5 MPa. C,D, Cured at 0.3 MPa. E,F, Cured at 0.1 MPa. G, Sample for void characterization [Colour figure can be viewed at wileyonlinelibrary.com]

distribution in a glass fibre reinforced polymer composite used in wind turbine blades; the fatigue mechanisms were also examined using computed tomography. M.A. Suhot and A.R. Chambers[5,6] explored the effect of voids on the flexural fatigue properties of unidirectional (UD) carbon fibre polymer composites used in the wind turbine industry, and they reported a general trend of increasing fatigue strength with decreasing porosity level. Sanjay Sisodia[7] investigated the effect of voids on the quasistatic and tension-tension (T-T) fatigue properties of HTS40/RTM6 laminated composite, and the results showed that the fatigue life of the composite was sensitive to the void content. Apart from the studies on the effect of voids alone, studies on fatigue behaviours of composites with void defect in certain environment have also been reported. A.Y. Zhang[10] investigated the effect of voids on the bending strength and bending fatigue of T300/914 laminated composite exposed to hygrothermal environment; they found that both the bending strength and bending fatigue performance of the material decreased with increasing level of porosity.

This study focuses on the characterization of the effect of voids on the T-T and compression-compression (C-C) fatigue of CFRP laminated composites. The characterization of voids was accomplished first, and the fatigue properties of composites were studied through the following aspects: (1) fatigue life, fatigue strength, and failure probability distribution of laminated composites; (2) residual stiffness degradation on the basis of the change of the hysteresis loop in the course of fatigue; (3) failure mechanisms based on the observation of crack initiation/propagation and SEM fractographic analysis; and (4) analytical fatigue model regarding the residual stiffness. We expect that the present investigation could be helpful in understanding the effect of voids on the fatigue of fibrous polymer laminated composites under different loading configurations and could serve as a guide line in the safety design in engineering applications.

2 | EXPERIMENTAL

2.1 | Materials

T300/924 laminated composite, as a commonly used CFRP composite, was fabricated and tested in this study. To control the void content in the epoxy matrix, different compression pressures (0.5, 0.3, and 0.1 MPa) were chosen in compression molding. The temperature in curing process first increases with a heating rate of 6°C/min and levels off at 180°C for 2 hours before cooling down. The stacking sequences of the plaques consist of $[0]_{12}$, , $[0]_{16}$, , $[90]_{12}$, , and $[0/\pm45/0/90]_s$, . The thickness of a single ply is approximately 0.14 mm. A digital microscopy image module was proposed in this study to examine

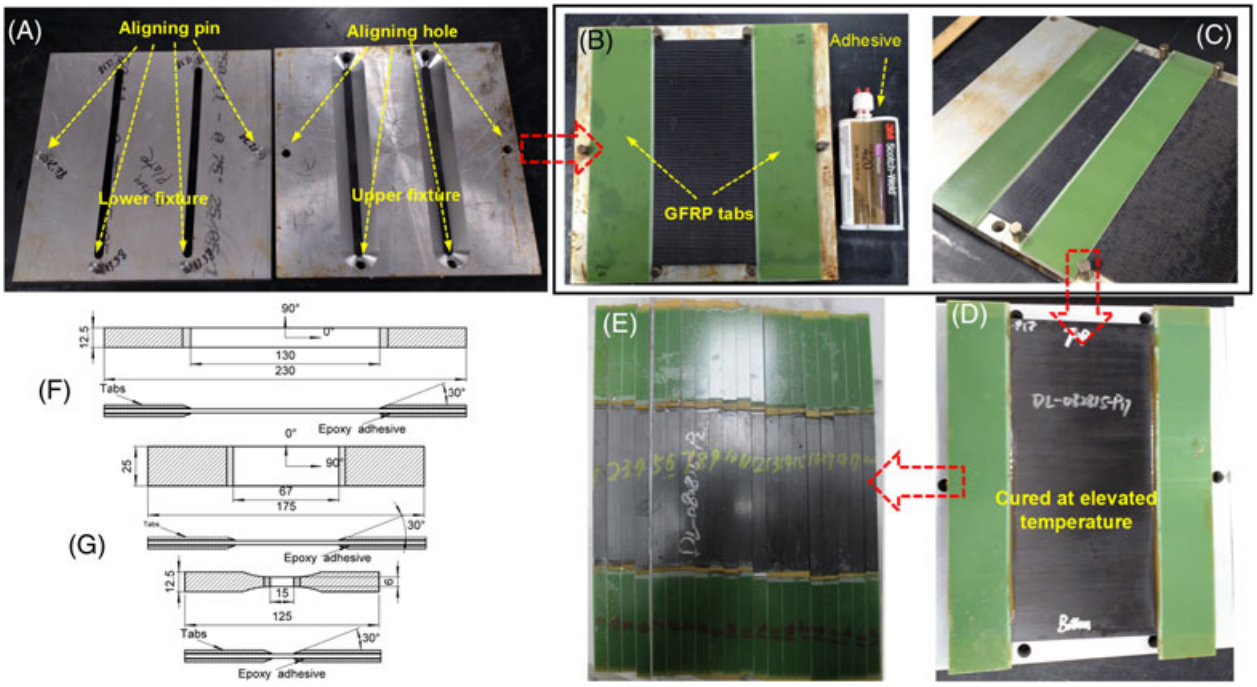

FIGURE 2 Tabbing process for composite plaques. A, Fixture. B, Plaque for tensile test and tension-tension (T-T) fatigue test. C, Plaque for compression test and compression-compression (C-C) fatigue test. D, Tabbed plaque with cured adhesive. E, Samples. F, Sample configurations for longitudinal/transverse T-T fatigue test. G, Sample configuration for C-C fatigue test [Colour figure can be viewed at wileyonlinelibrary.com]

the void content, morphology of voids, and the fibre volume fraction (the detailed curing process, manufacturing parameters, and properties of the fibers and the matrix can be found in Figure S1 and Tables S1 and S2).

2.2 | Porosity characterization

The samples for porosity characterization, with dimensions of 10 mm ×, 10 mm, were cut from the composite

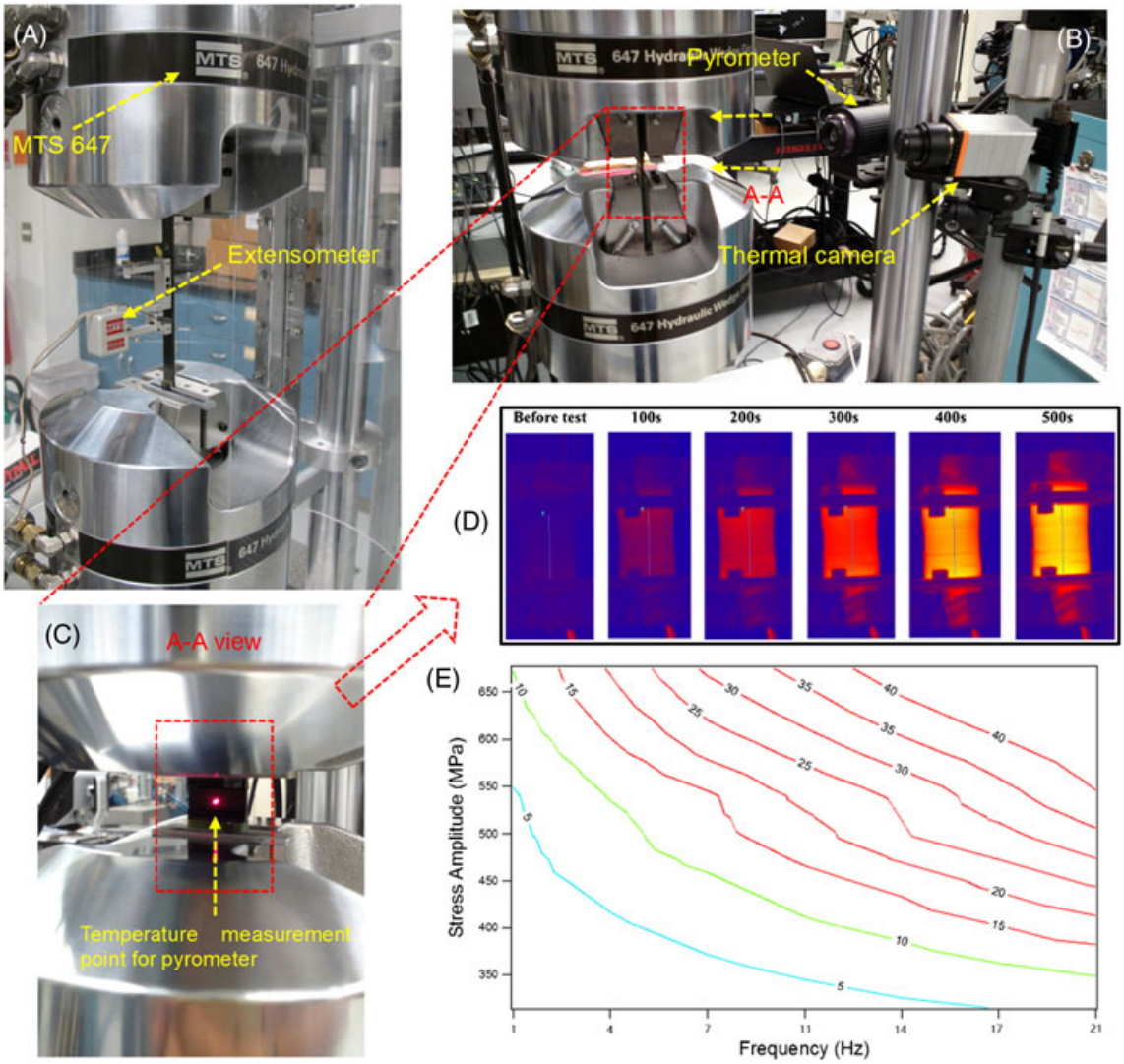

FIGURE 3 Configurations of the test frame. A, Experimental set-up for quasistatic tensile and tension-tension fatigue tests. B, Experimental set-up for compression-compression fatigue test with temperature measurement system. C, Temperature measurement by pyrometer. D, Thermal images of the sample's profile. E, Iso-temperature-rise curves at various frequencies and loading levels (/°C,) [Colour figure can be viewed at wileyonlinelibrary.com]

TABLE 1 Void content of plaques cured under different compression pressures

Panel No.	Sample Lay-up	Compression Pressure, MPa	Void Content
UD-P16	$[0]_{16}$,	0.5	0.8%
UD-P12A	$[90]_{12}$,	0.5	0.7%
UD-P12B	$[0]_{12}$, , $[90]_{12}$,	0.3	2.2%
UD-P12C	$[0]_{12}$, , $[90]_{12}$,	0.1	4.0%
MD-PA	$[0/\pm 45/0/90]_s$,	0.5	0.6%
MD-PB	$[0/\pm 45/0/90]_s$,	0.1	3.8%

Abbreviations: MD, multidirectional; UD, unidirectional.

plaques using a water jet. These samples were first embedded in epoxy resin and cured for 24 hours; the cross sections were then prepared by abrasive papers and synthetic diamond compounds. To obtain clear microimages of the samples, an optical microscope with a complementary metal oxide semiconductor (CMOS) camera connected to a computer was used in this article. For the purpose of providing a statistically representative data set, 5 samples were prepared for each plaque, and 3 images per sample were examined. To reduce the system error, the positions of samples on the plaques were randomly selected. Some typical microimages of the samples cured at different compression pressures are shown in Figure 1.

2.3 | Testing configuration

In accordance with ASTM D3039, rectangular samples with various geometries were used in this study. To protect the gripping section, glass fibre reinforced polymer composite tabs were attached to both ends of the samples. The tabs were attached to the samples by Epoxy Adhesive 3M DP420, which is capable of providing adequate shear strength after being cured at 150°C for 15 hours according to our test results. Specific fixtures were manufactured to hold the tabs in position and to provide essential pressure when the adhesive was cured in the oven. The preparation and configurations of samples are shown in Figure 2.

All the tests were conducted in an MTS 647 hydraulic servo dynamic testing machine, and the configurations of the tests are shown in Figure 3. The quasistatic tensile tests and compression tests were performed under displacement control with displacement rate equalled 1 mm/min, while the fatigue tests were performed under load control. In the tensile tests, 5 samples were tested for laminate with given lay-up and void content. The axial strain was captured by an extensometer (MTS E 634.31F-24) (the detailed quasistatic tensile test data can be found in Table S4). To avoid the impact of high temperature as a result of the high

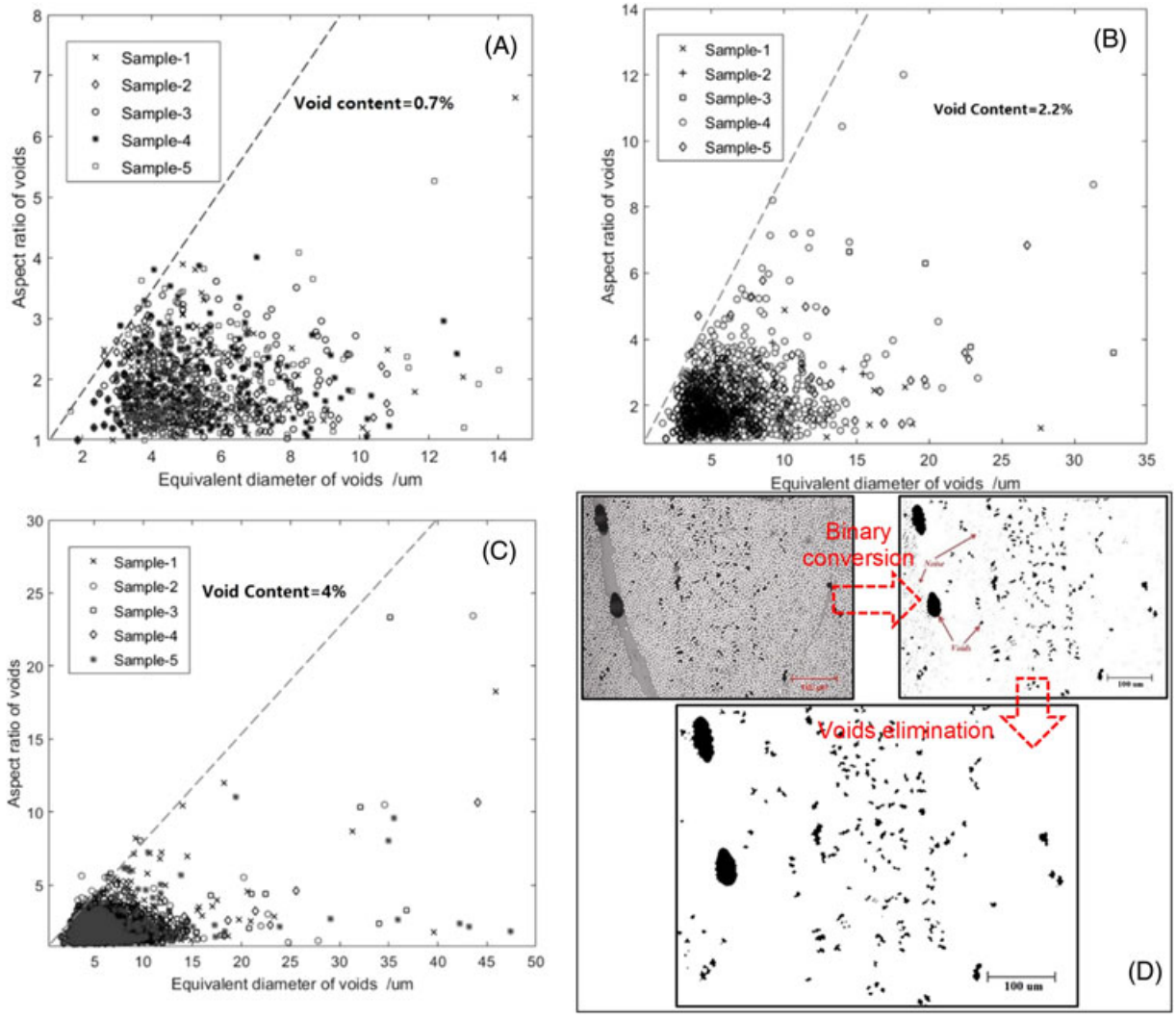

FIGURE 4 Void morphology analysis: aspect ratio versus equivalent diameter of voids for samples with voids at, A, 0.7%; B, 2.2%; and, C, 4%. D, Image processing for void characterization [Colour figure can be viewed at wileyonlinelibrary.com]

loading frequency and high loading level in fatigue tests, temperature measurement for short rectangular specimens was conducted to determine a proper loading frequency. A thermal camera, as shown in Figure 3B-D, was used to monitor the temperature change on the surface of the sample, assisted by a pyrometer as validation. The temperature of the sample would increase at the beginning of the test and reach a steady state after certain number of cycles. In this article, the steady-state temperatures at different loading frequencies and loading levels were recorded, and isotemperature-rise curves were drawn (Figure 3E). According to the test results, a frequency of 7 Hz was selected to avoid high temperature as well as to guarantee an acceptable test speed. The load ratio $R, = 0.1$ was used in the T-T fatigue tests and $R, = 10$ in C-C fatigue tests. The Young modulus degradation of the sample was traced with the help of the evolution of secant slope of the hysteresis loop.

In addition, to investigate the effect of voids on the fatigue deterioration of the composite under T-T fatigue loading, transverse crack density evolution was studied by measuring the crack density at both lateral surfaces of the specimen. In this study, the evolution of crack density was examined based on optical microimages by interrupting the fatigue tests at certain stages.

3 | RESULTS AND DISCUSSIONS

3.1 | Void characterization

Samples from plaques cured at various compression pressures were examined to determine the void content. Table 1 presents the resulting averaged void content of each plaque. The detailed void content measurement results can be found in Table S3 and Figure S2.

Figure 4A-C demonstrates the distribution of aspect ratio versus the equivalent diameter of voids in 12-ply UD plaques cured under 0.5, 0.3, and 0.1 MPa, respectively. It is clear that for all 3 plaques, most of the points lie on the right side of the dashed line, which suggests that smaller voids tend to be closer to spherical. According to Figure 1, the interlaminar voids, which usually derive from the entrapped air during autoclaving, are usually larger in size and have a higher average aspect ratio compared to intralaminar voids, which usually come from the volatiles that derive from the chemical reactions during the manufacturing process. These larger and more irregular voids may play a crucial role to accelerate the initiation and propagation of cracks when subjected to cyclic loading.

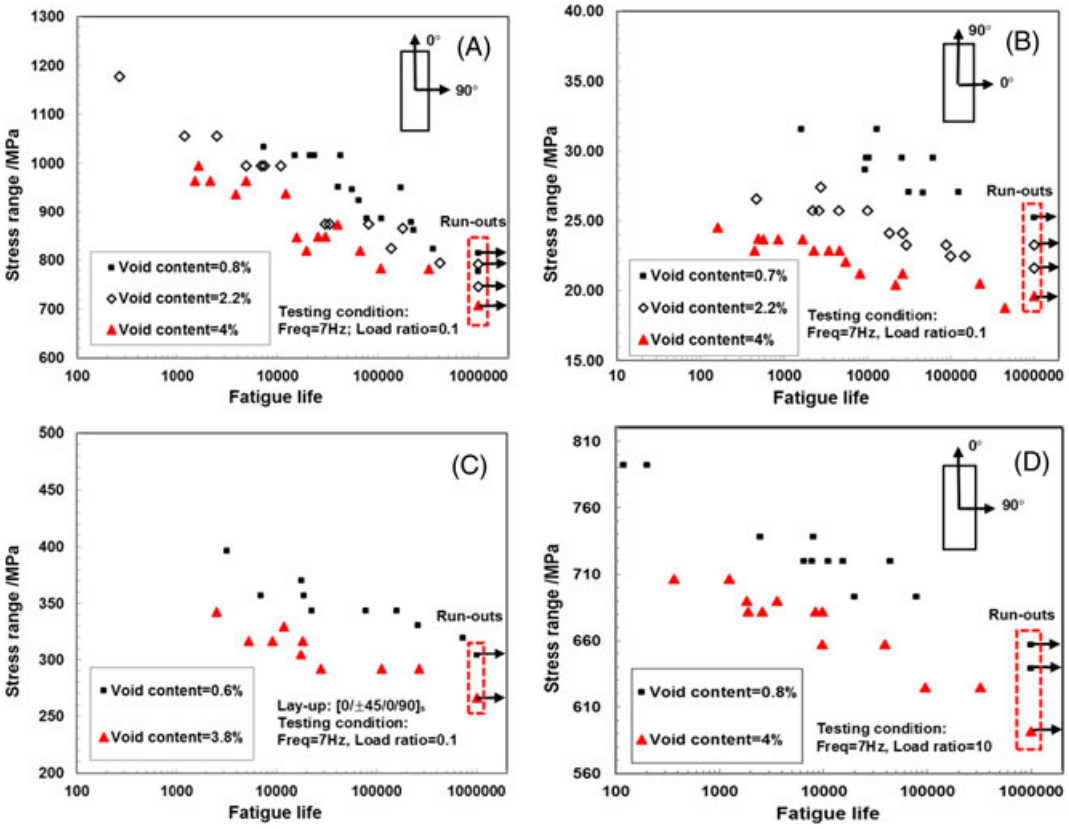

FIGURE 5 S-N diagrams of composite laminates at different porosity levels. A, Unidirectional (UD) laminates subjected to longitudinal tension-tension (T-T) cyclic loading. B, UD laminates subjected to transverse T-T cyclic loading. C, multidirectional laminates with lay-up $[0/\pm 45/0/90]_s$, . D, UD laminates subjected to longitudinal compression-compression cyclic loading [Colour figure can be viewed at wileyonlinelibrary.com]

3.2 | Fatigue life assessment

Tension-tension fatigue tests were performed for UD composites in longitudinal/transverse direction and for multidirectional (MD) laminates with a stacking sequence of $[0/\pm45/0/90]_s$, , while C-C tests were performed for UD laminates in longitudinal direction. The specimens were subjected to different stress levels corresponding to various fractions of ultimate tensile strength or compression stress. For both the UD and the MD laminates, failure of specimen was programmed in the test machine as complete fracture. However, the failure of the MD specimens is different as compared to that of the UD specimens. To be specific, for the longitudinal UD laminates, no obvious damage could be seen prior to fracture. Specimens split suddenly at final failure, with numerous debris burst out; due to vast amount of delamination and fibre-matrix interfacial debonding, no clear fracture surfaces could be observed, whereas for the MD specimens, large amount of interply failures could be seen before final failure. Besides, plies with different fibre orientations have different failure modes: for 0° plies, fibre breakage and interfacial debonding are the dominant failure modes; whereas for ±45° and 90° plies, cracks propagate along the fibre

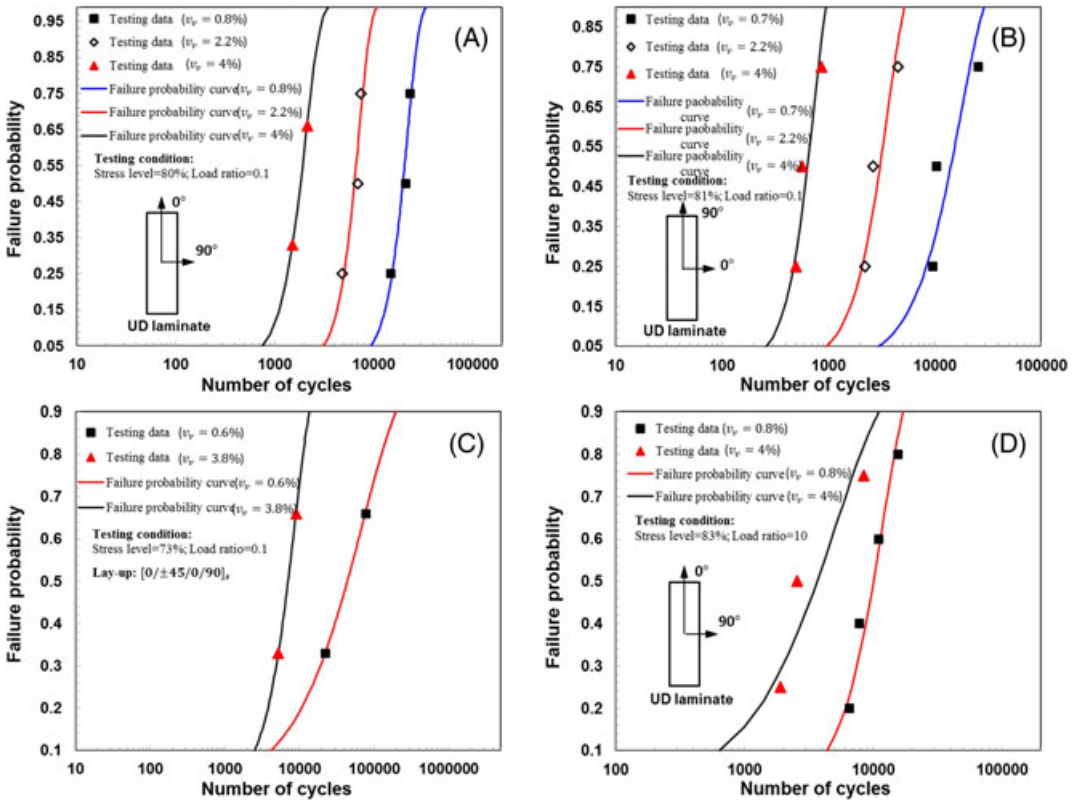

FIGURE 6 Failure probability of composite laminates based on Weibull distribution. A, In the case of unidirectional (UD) laminates under longitudinal tension-tension (T-T) loading. B, In the case of UD laminates under transverse T-T loading. C, In the case of laminates with lay-up $[0/\pm45/0/90]_s$, under T-T loading. D, In the case of UD laminates under longitudinal compression-compression fatigue loading [Colour figure can be viewed at wileyonlinelibrary.com]

TABLE 2 Fitting parameters of fatigue failure probability curve model

Testing Material	UD Laminate (Longitudinal)			UD Laminate (Transverse)			MD Laminate $[0/\pm45/0/90]_s$,		UD Laminate (Longitudinal)	
Stress ratio R	$R = 0.1$								$R = 10$	
Stress level u,	80%			81%			73%		83%	
Void content	0.8%	2.2%	4%	0.7%	2.2%	4%	0.6%	3.8%	0.8%	4%
η,	22 026	7115	2071	17 659	3594	720	69 564	8639	11 778	5115
λ,	3.48	3.58	2.94	1.67	2.26	2.95	0.80	1.82	2.27	1.09

Abbreviations: MD, multidirectional; UD, unidirectional.

orientation, and severe interfibre bundle failures and fibre-matrix interfacial debonding can be observed.

The effect of voids on the fatigue behaviours of the composite was first assessed in terms of fatigue life. Figure 5A,B depicts the S-N diagrams for T-T fatigue tests of UD laminates in longitudinal and transverse directions, respectively. The fatigue life decreases almost linearly as the stress level increases. It is evidently clear that for the UD laminated composites, increase of void content would always lead to decrease of fatigue life when subjected to T-T cyclic loading. Meanwhile, a lower fatigue strength can be found for materials with higher porosity level as well, both for longitudinal and transverse directions. In addition, the transverse fatigue resistance is more sensitive to the porosity level (Figure 5B). Given the dominant failure mode in the transverse test is matrix cracking rather than fibre breakage, it is reasonable to assume that the presence of voids has a more significant impact on the matrix-dominated mechanical properties of the fibrous composites.

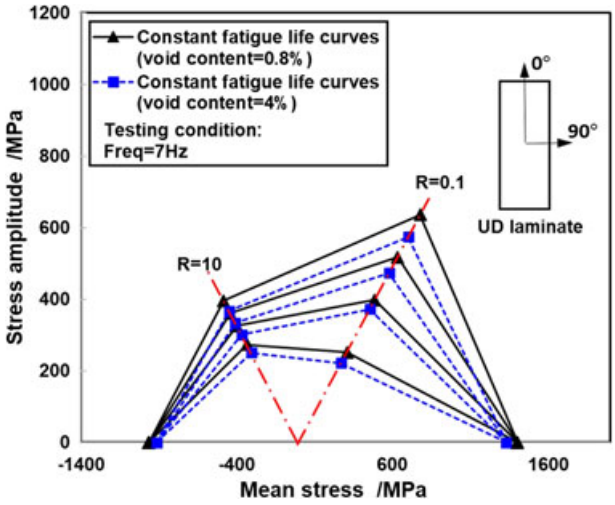

FIGURE 7 Constant fatigue life diagram of unidirectional (UD) laminates at porosity level of 0.8% and 4% [Colour figure can be viewed at wileyonlinelibrary.com]

Similar effect of voids can be observed for MD laminates with a stacking sequence of $[0/\pm45/0/90]_s$, subjected to T-T fatigue loading and UD laminates subjected to C-C loading, where the S-N curve seems to experience a translational displacement as the porosity level increases (Figure 5C,D). However, the C-C fatigue of UD laminates seems to be more sensitive to the stress level compared with the T-T fatigue (the detailed experimental data of the fatigue tests are presented in Tables S5-S8). Finally, tests for poolability showed that the individual data sets in each figure cannot be pooled.

In an attempt to evaluate the fatigue discreteness of the laminated composites and to assess the durability of the material in terms of the failure probability, a 2-

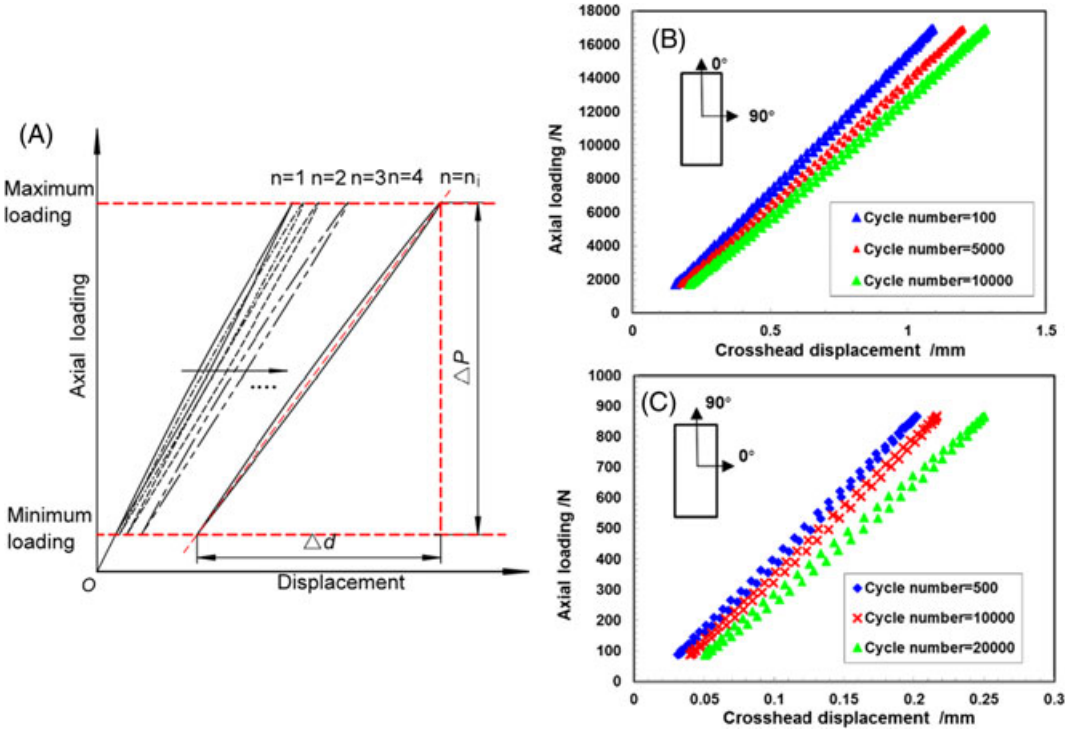

FIGURE 8 Hysteresis loops evolution of laminated composites. A, Schematic of evolution of hysteresis loops with respect to number of cycles and hysteresis loops evolution of, B, the longitudinal fatigue test and, C, transverse fatigue test for unidirectional laminates [Colour figure can be viewed at wileyonlinelibrary.com]

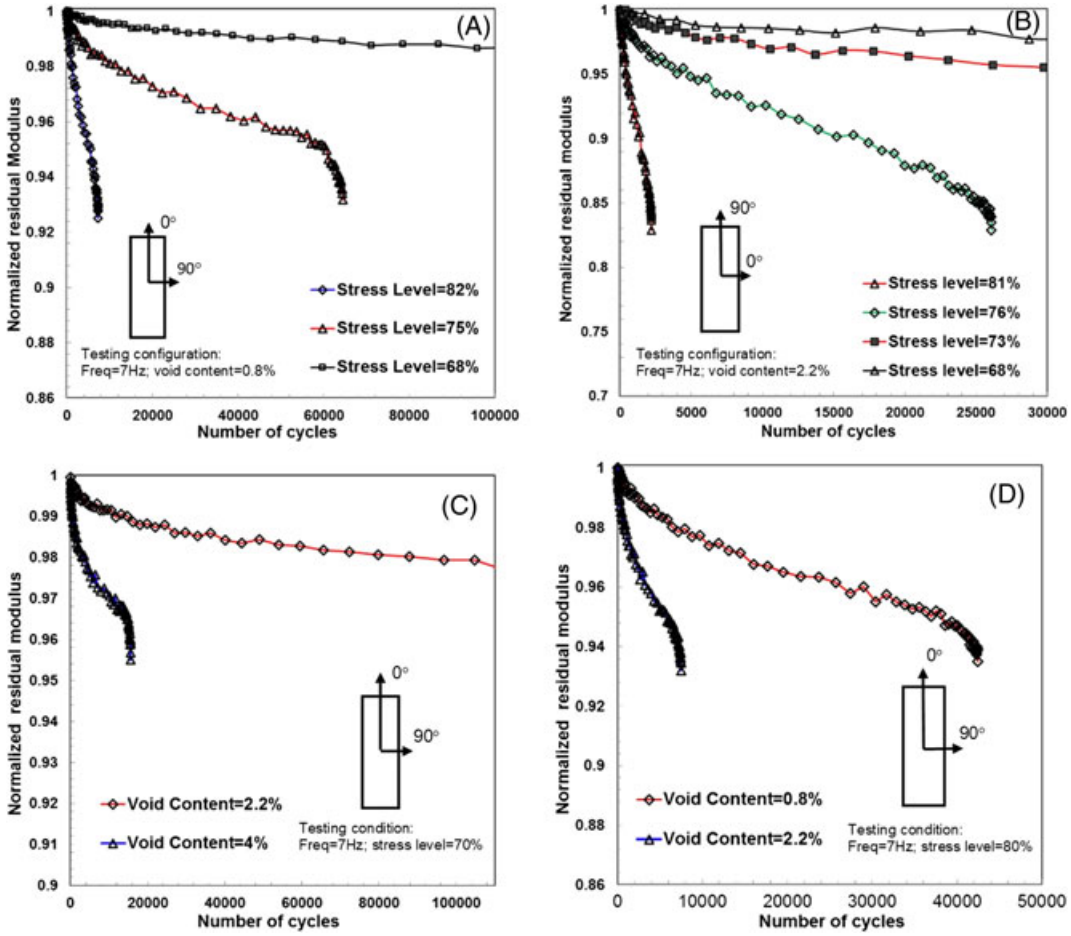

FIGURE 9 Stiffness degradation versus number of cycles. A,B, Laminates with certain void content at various stress levels and laminates with various void content at given load level of, C, 70% and, D, 80% [Colour figure can be viewed at wileyonlinelibrary.com]

parameter Weibull distribution function was used in this study (Equation A1). Figure 6 presents the failure probabilities and the predictive results for UD laminates under longitudinal/transverse T-T fatigue loading, MD laminates under T-T fatigue loading, and UD laminates under longitudinal C-C fatigue loading. The fitting parameters can be found in Table 2. A good correlation can be observed between the failure probability and the number of cycles.

By plotting the test data on the mean stress-stress amplitude plane, a constant fatigue life diagram for UD laminate was drawn to take both the effect of voids and effect of mean stress into account (Figure 7). The fatigue life at certain stress level, porosity level, and stress ratio was obtained by interpolation based on a simple $S-N_f$, fatigue model (Equation A3).

3.3 | Stiffness degradation

The fatigue damage of composites can be evaluated in terms of the degradation of macroscopically measurable properties such as residual stiffness or strength. Compared to residual strength, the usage of residual stiffness

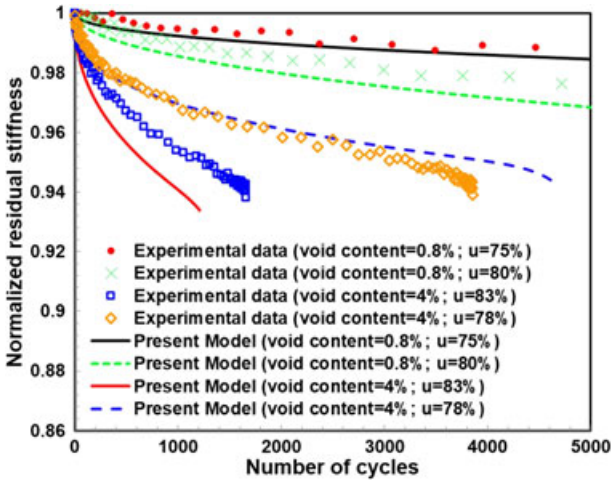

FIGURE 10 Predictive stiffness degradation versus cycles for unidirectional laminates at various stress levels and porosity levels. Here, the fatigue model is related to Equations A3 and A7 [Colour figure can be viewed at wileyonlinelibrary.com]

as a detector of the damage induced by the cyclic loading has advantages due to its non-destructive nature and smaller scatter. In this study, the dynamic stiffness degradations of samples subjected to T-T fatigue loadings were analysed through the same method described in literature.[22] The degradation of residual modulus was extracted on the basis of the secant slope of the line segment between the maximum of minimum points of each cycle (Figure 8A). Figure 8B,C shows the hysteresis loops at certain cycles for UD composites subjected to fatigue loadings in the longitudinal and transverse directions, respectively. Obvious translational displacement and rotation of the hysteresis loop can be observed as the number of cycles increases.

Normalized stiffness degradations for UD laminates under cyclic loading in longitudinal and transverse directions are shown in Figure 9A and 9B, respectively. As shown in the figures, higher stress levels are accompanied by faster stiffness reduction processes (eg, for laminates with void content of 0.8%, the sample tested at stress level of 82% experienced a more rapid axial modulus decrease with respect to the number of cycles as compared with that of samples tested at stress levels of 75% and 68%). Moreover, higher load levels corresponding to a larger decrease in moduli were also observed, which is consistent with the analytical results of Gowayed[23] based on shear lag theory.

The evaluations of effect of voids for laminates subjected to given stress levels are presented in Figure 9 C,D. According to the figure, the presence of voids is able to significantly accelerate the fatigue damage accumulation process in both cases. As void content increases, the axial modulus decreases more rapidly up to fracture occurs, thus leading to a shorter fatigue life. However, the modulus drop for laminates with different void contents at rupture seems not to be affected by the presence of voids, as shown in Figure 9D.

For the purpose of quantitatively assessing the effect of voids on the fatigue behaviours of composites and to provide a method to predict the fatigue life of components during components design, a simple predictive method was deduced on the basis of the stiffness degradation of composites at various porosity levels (Equation A6). By using quadratic polynomial equations, the functions δ, , φ_1, , and φ_2, can be well fitted with the correlation coefficients ranging from 0.926 to 0.971. The results pertaining to the fitting curves are presented in Figure 10. A good correlation can be observed between the test data and the fitting results.

3.4 | Damage evaluation through crack density measurement

For composites subjected to T-T fatigue loading, stiffness variation can be attributed to matrix cracking. To explain the effect of voids on the fatigue mechanisms of composites under T-T loading, matrix cracks on the free edges of the UD laminates were assessed at specified cycles using an optical microscope. Figure 11A shows the microscopic images of matrix cracks at various stages of the fatigue, while Figure 11B shows the evolution of matrix crack density for laminates at various stress levels and porosity levels. According to Figure 11A, matrix cracks

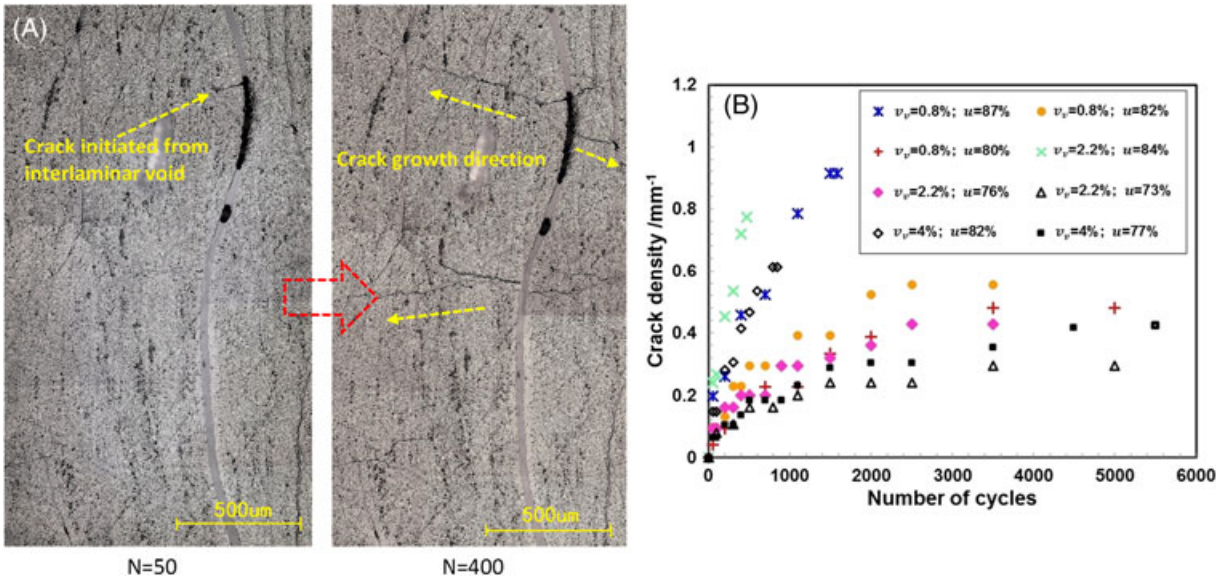

FIGURE 11 Fatigue process of unidirectional laminates under tension-tension fatigue loading. A, Images of initiation of matrix cracks from interlaminar voids at specified cycles. B, Evolution of crack density for 90°, laminates at different porosity levels and stress levels [Colour figure can be viewed at wileyonlinelibrary.com]

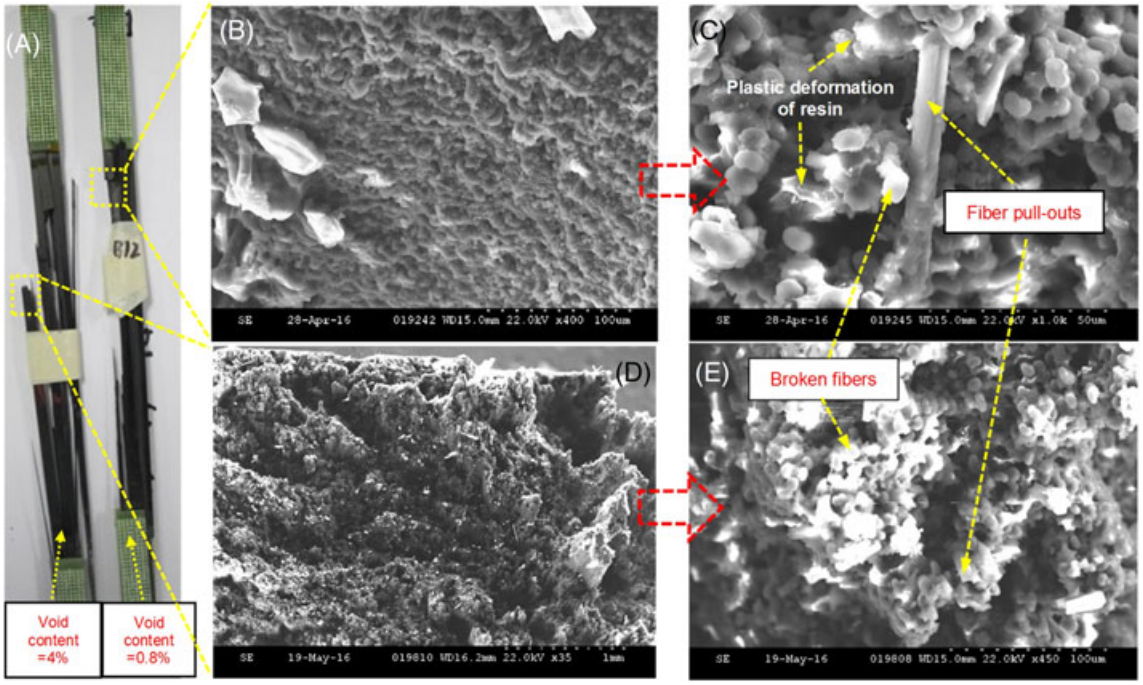

FIGURE 12 Images of fracture surfaces of specimens with void content at 0.8% and 4%. A, Specimens that failed under tension-tension fatigue loading and scanning electron microscope images of fracture morphology of, B,C, specimen with void content at 0.8% and, D,E, specimen with void content at 4% [Colour figure can be viewed at wileyonlinelibrary.com]

are apt to nucleate from interlaminar voids and propagate into the ply, indicating a faster crack initiation/propagation. The results are consistent to the crack density measurement results shown in Figure 11B. For laminates with higher void content, matrix cracks would reach saturation state in fewer cycles. However, the saturation of matrix cracks seems not to be associated with the porosity level. To conclude, the presence of voids would accelerate the fatigue of CFRP composites by stimulating the evolution of matrix cracks.

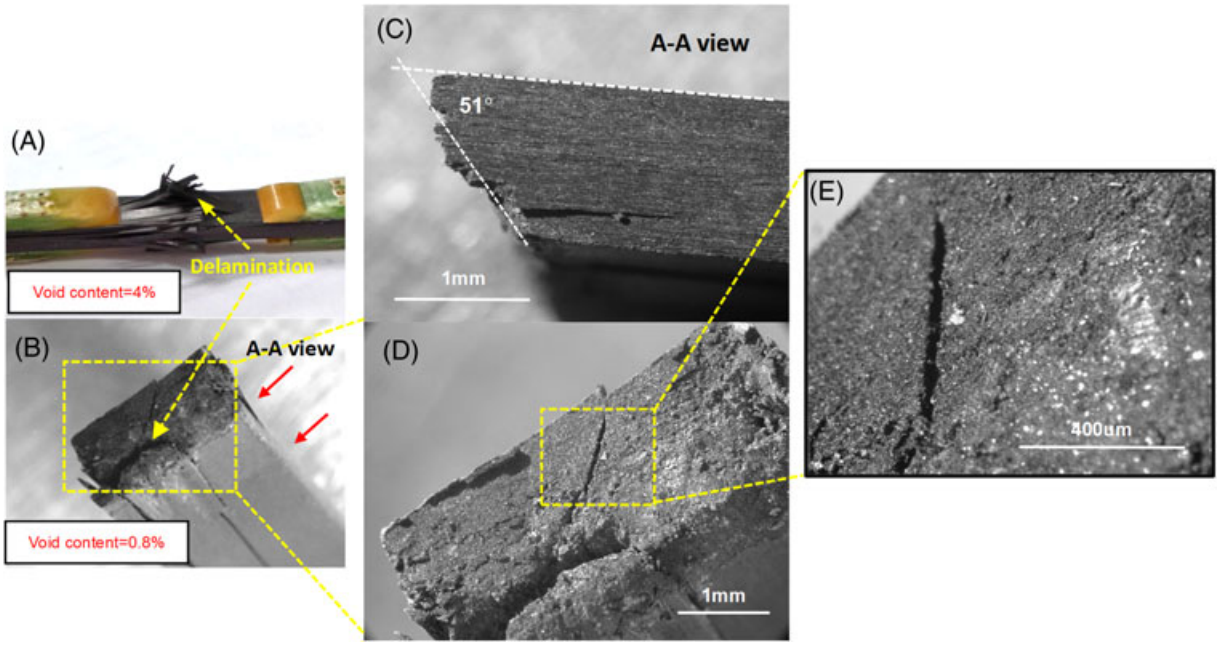

FIGURE 13 Images of fracture surfaces of specimens with void content at 0.8% and 4%. A,B, Specimens that failed under compression-compression fatigue loading. C-E, Images of fracture morphology of specimen with void content of 0.8% [Colour figure can be viewed at wileyonlinelibrary.com]

3.5 | Fatigue fractographic analysis

Aside from the crack density measurement during the course of fatigue, the fractographic analysis was also performed as a supplemental approach to further reveal the effect of voids on the fatigue failure mechanisms of composites. The postfailure modes and fracture morphology of the longitudinal UD specimens with various void contents are shown in Figure 12. Intriguingly, although the presence of voids, as shown in the previous section, would shorten the fatigue life of composites by stimulating the matrix cracks to nucleate and propagate, specimens with 0.8% and 4% voids share similar features of fractures. Large amount of delamination (Figure 12A), fibre pull-outs, broken fibers, and matrix plastic deformation (Figure 12C,E) can be observed. However, subtle differences can still be found in mesoscale SEM images of the fracture surfaces. Owing to a higher level of porosity, matrix cracks in laminates with higher void content may tend to deflect into fibre orientation to form fibre-matrix interface damage, thereby resulting in "rougher" crack surfaces (Figure 12B,D).

Despite specimens with different void contents share fairly similar characteristics for T-T fatigue fracture surfaces, in C-C fatigue tests, a clear discrepancy can be observed in fracture morphology of laminates at various porosity levels (Figure 13). Relative flat fracture surfaces were found for specimens with void content of 0.8% (Figure 13B), whereas "brush-like" fracture surfaces were observed for specimens with void content of 4% (Figure 13 A). The "brush-like" feature can be attributed to vast amount of interfibre bundle failure including delamination owing to the presence of voids. As discovered in the previous study, the voids, as inherent defects of the material, could stimulate the matrix crack in the material when subjected to T-T fatigue loading. Similarly, interphase failure may tend to initiate from the voids as well under C-C cyclic loading, and the formation of fibre-matrix interface failure and delamination could trigger the unstable failure of fibers at early stage of fatigue, thus leading to fewer cycles to failure. Although there was also delamination occurred in composites with lower void content (Figure 13D,E), the fracture surfaces were relatively flat, with an angle formed (approximately 51°, , Figure 13C) with respect to the fibre direction.

4 | CONCLUSIONS

By performing the fatigue testing and the relative analysis for T300/924 laminated composites at various porosity levels, this work successfully evaluated the effects of voids on their T-T and C-C fatigue behaviours, alongside the initiation/propagation of matrix cracks and fatigue failure mechanisms. The fatigue behaviours of the composite displayed a high dependency on the void content when subjected to both T-T and C-C loading. The relationship between applied stress level and the corresponding fatigue life was correlated by a semilogarithmic linear model, with the slope and intercept of the fitted curves described as functions of void content to capture the voids-induced effects. Apart from fatigue life, the effect of voids showed different mechanisms for T-T and C-C fatigue failure of the composite. To be specific, for specimens under T-T cyclic loading, revealed by the matrix crack density measurement results, the presence of voids could stimulate matrix cracks to initiate and propagate, resulting in more rapid damage accumulation and stiffness reduction process, whereas for specimens under C-C cyclic loading, voids seem to play a different role in fatigue of composites. By stimulating failures including the interphase failure and delamination to occur, the presence of voids would lead to earlier unstable fibre fracture as well as fewer cycles to failure. Lastly, a residual stiffness model and a probability failure model were established from the engineering perspective. The results of the work provided a comprehensive insight for fatigue behaviours of CFRP laminated composites under the influence of voids. The understanding of the effect of voids along with the related numerical models, which have taken the effect of voids into account, will be useful for the future engineering applications of laminated polymer composites with void defects.

ORCID

H. Liu http://orcid.org/0000-0002-0762-2828

REFERENCES

1. Garbo SP, Ogonowski JM. Effect of variances and manufacturing tolerances on the design strength and life of mechanically fastened composite joints. AFWAL-TR-81-3041 1981, vol. 1.
2. Prakash R. Significance of defects in the fatigue failure of carbon fibre reinforced plastics. *Fibre Sci Technol*. 1981;14:171-181.
3. de Almeida SFM, Neto ZSN. Effect of void content on the strength of composite laminates. *Compos Struct*. 1994;28(2):139-148.
4. Lambert J, Chambers AR, Sinclair I, Spearing SM. 3D damage characterisation and the role of voids in the fatigue of wind turbine blade materials. *Compos Sci Technol*. 2012;72(2):337-343.
5. Suhot MA, Chambers AR. The effect of voids on the flexural fatigue performance of unidirectional carbon fibre composites. 16th Int Conference on Composite Materials, Kyoto, Japan, 2007.

6. Chambers AR, Earl JS, Squires CA, Suhot MA. The effect of voids on the flexural fatigue performance of unidirectional carbon fibre composites developed for wind turbine applications. *Int J Fatigue*. 2006;28:1389-1398.
7. Sisodia S, Gamstedt EK, Edgren F, Varna J. Effects of voids on quasi-static and tension fatigue behaviour of carbon-fibre composite laminates. *J Compos Mater*. 2015;49(17):2137-2148.
8. Protz R, Kosmann N, Gude M, Hufenbach W, Schulte K, Fiedler B. Voids and their effect on the strain rate dependent material properties and fatigue behaviour of non-crimp fabric composites materials. *Compos Part B-Eng*. 2015;83:346-351.
9. Schmidt F, Rheinfurth M, Horst P, Busse G. Multiaxial fatigue behaviour of GFRP with evenly distributed or accumulated voids monitored by various NDT methodologies. *Int J Fatigue*. 2012;43:207-216.
10. Zhang A, Li D, Lu H, Zhang D. Qualitative separation of the effect of voids on the bending fatigue performance of hygrothermal conditioned carbon/epoxy composites. *Mater Des*. 2011;32(10):4803-4809.
11. Bathias C. An engineering point of view about fatigue of polymer matrix composite materials. *Int J Fatigue*. 2006;28:1094-1099.
12. Song J, Wen WD, Cui HT, Liu HL, Xu Y. Effects of temperature and fiber volume fraction on mechanical properties of T300/QY8911-IV composites. *J Reinf Plast Comp*. 2014;34(2):157-172.
13. Allah MH, Abdin EM, Selmy AI, Khashaba UA. Effect of fibre volume fraction on the fatigue behaviour of GRP pultruded rod composites. *Compos Sci Technol*. 1996;56(1):23-29.
14. Huang X. Fabrication and properties of carbon fibers. *Materials*. 2009;2(4):2369-2403.
15. Hu Y, Lang AW, Li X, Nutt SR. Hygrothermal aging effects on fatigue of glass fiber/polydicyclopentadiene composites. *Polym Degrad Stab*. 2014;110:464-472.
16. Zhang JY, Sun CQ, Zhao LB, Fei BJ. Experiment research of environment effects on fatigue life of carbon/bismaleimide composite laminates with central hole. *Key Eng Mater*. 2011;452-453:525-528.
17. Liu L, Zhang BM, Wang DF, Wu ZJ. Effects of cure cycles on void content and mechanical properties of composite laminates. *Compos Struct*. 2006;73:303-309.
18. Koushyar H, Alavi-Soltani S, Minaie B, Violette M. Effects of variation in autoclave pressure, temperature, and vacuum-application time on porosity and mechanical properties of a carbon fiber/epoxy composite. *J Compos Mater*. 2011;46(16):1985-2004.
19. Liebig WV, Viets C, Schulte K, Fiedler B. Influence of voids on the compressive failure behaviour of fibrereinforced composites. *Compos Sci Technol*. 2015;117:225-233.
20. Selmi A. Void effect on carbon fiber epoxy composites. 2nd International Conference on Emerging Trends in Engineering and Technology (ICETET'2014), London, May 30–31, 2014.
21. Costa ML, de Almeida SM, Rezende MC. The influence of porosity on the interlaminar shear strength of carbon/epoxy and carbon/bismaleimide fabric laminates. *Compos Sci Technol*. 2001;61:2101-2108.
22. Bensadoun F, Vallons KAM, Lessard LB, Verpoest I, Van Vuure AW. Fatigue behaviour assessment of flax–epoxy composites. *Compos Pt A Appl Sci Manuf*. 2016;82:253-266.
23. Gowayed Y, Ojard G, Santhosh U, Jefferson G. Modeling of crack density in ceramic matrix composites. *J Compos Mater*. 2015;49(18):2285-2294.
24. Shokrieh MM, Lessard LB. Progressive fatigue damage modeling of composite materials, part I: modeling. *J Compos Mater*. 2000;34:1056-1080.
25. Shokrieh MM, Lessard LB. Progressive fatigue damage modeling of composite materials, part II: material characterization and model verification. *J Compos Mater*. 2000;34:1081-1116.
26. Harris B, Gathercole N, Lee JA, Reiter H, Adam T. Life-prediction for constant-stress fatigue in carbon-fibre composites. *Phil Trans R Soc Lond A*. 1997;355:1259-1294.
27. Reifsnider K. Fatigue behavior of composite materials. *Int J Fract*. 1980;16(6):563-583.
28. Jamison RD. *Advanced Fatigue Damage Development in Graphite Epoxy Laminates*. Fort Belvoir, VA: Defense Technical Information Center; 1982.
29. Mao H, Mahadevan S. Fatigue damage modelling of composite materials. *Compos Struct*. 2002;58:405-410.

SUPPORTING INFORMATION

Additional Supporting Information may be found online in the supporting information tab for this article.

How to cite this article: Liu H, Cui H, Wen W, Kang H. Fatigue characterization of T300/924 polymer composites with voids under tension-tension and compression-compression cyclic loading. *Fatigue Fract Eng Mater Struct*. 2018;41:597–610. https://doi.org/10.1111/ffe.12721

APPENDIX A.

A.1. | $p-S-N_f$ model

The Weibull distribution used in this article is shown in Equation A1, in which the 2 parameters $\eta(u)$, and $\lambda(u)$, represent the scale and shape parameters, respectively. Here, the stress level u, is defined as the ratio of the maximum stress and the ultimate tensile strength (in T-T tests) or ultimate compression stress (in C-C tests).

$$P(n_i) = 1-\exp\left(-\left(\frac{n_i}{\eta(u)}\right)^{\lambda(u)}\right). \quad \text{(A1)}$$

In this equation, i, stands for the serial number of the sample and $P(n_i)$, is the failure probability of the no. i,

sample. The scale and shape parameters can be obtained by transforming Equation A1 into the following equation.

$$\ln(n_i) = \frac{1}{\lambda}\ln(-\ln(1-P(n_i))) + \ln(\eta). \quad \text{(A2)}$$

The parameters can then be obtained through linear regression on the basis of the test data.

A.2. | $S-N_f$, model

The $S-N_f$, model used in this article was based on the model proposed by Shokrich[24,25] and Harris.[26] As shown in the S-N diagram, translational displacement and rotation can be observed in the S-N curve for laminates at different porosity levels. To take the effect of voids into account, the constants in the conventional model are replaced by the function of void content. The modified expression is as shown in Equation A3.

$$u' = \frac{\ln(a/f)}{\ln[(1-q)(c+q)]} = \gamma(v_v) + k(v_v)\lg N_f. \quad \text{(A3)}$$

In this equation, $a=(\sigma_{max}-\sigma_{min})/2[\sigma_t],$, $q=(\sigma_{max}+\sigma_{min})/2[\sigma_t],$, $c=[\sigma_c]/[\sigma_t],$, $[\sigma_t]$, is the tensile strength, and $[\sigma_c]$, is the compression strength. f, is a constant. $\gamma(v_v)$, and $k(v_v)$, are functions of $v_v,$. $\gamma(v_v)$, is the intercept of the S-N curve with the vertical axis, while $k(v_v)$, is the slope of S-N curve.

A.3. | Residual stiffness model

The fatigue damage of composites was assessed by a damage index based on the stiffness variations in previous research[27,28] (Equation A4).

$$D = \frac{E_0 - E(N)}{E_0 - E(N_f)}. \quad \text{(A4)}$$

In this equation, E_0, indicates the initial modulus without damage, $E(N)$, indicates the residual modulus of the N^{th}, cycle, and N_f, is the fatigue life.

H. Mao[29] proposed a classic residual stiffness model for fibrous composites, as shown in Equation A5, the model well reflected the 3-stage characteristic of the stiffness degradation in the course of fatigue process. In the equation, $q,$, $m_1,$, and m_2, are independent parameters ($m_1<1,$, $m_2>1,$). The first term in the equation captures the rapid stiffness reduction at the beginning, while the second term describes the damage accumulation at the end of the fatigue process.

$$D = q\left(\frac{n}{N_f}\right)^{m_1} + (1-q)\left(\frac{n}{N_f}\right)^{m_2}. \quad \text{(A5)}$$

Here, for the purpose of capturing the effect of voids, the shape parameters were further defined as functions of void content and stress level (Equation A6).

$$D = A\delta(u,v_v)\left(\frac{N}{N_f}\right)^{\varphi_1(u,v_v)} + (1-A\delta(u,v_v))\left(\frac{N}{N_f}\right)^{\varphi_2(u,v_v)}. \quad \text{(A6)}$$

In this equation, A, is a constant associated with the material. $\delta,$, $\varphi_1,$, and φ_2, are functions of u, and $v_v,$. The expression of the functions can be obtained through curve fitting of the stiffness degradation data from the tests. Actually, the fatigue life can be straightly predicted by Equation A7 once the relative residual stiffness is measured.

$$\frac{E(N)}{E_0} = 1-\left(1-\frac{E(N_f)}{E_0}\right)\left[A\delta(u,v_v)\left(\frac{N}{N_f}\right)^{\varphi_1(u,v_v)} + (1-A\delta_1(u,v_v))\left(\frac{N}{N_f}\right)^{\varphi_2(u,v_v)}\right]. \quad \text{(A7)}$$